Free-Energy Profile of Small Solute Molecules at the Free Surfaces of Water and Ice, as Determined by Cavity Insertion Widom Calculations

Lívia B. Pártay and Pál Jedlovszky*

Laboratory of Interfaces and Nanosize Systems, Institute of Chemistry, Eötvös Loránd University, Pázmány Péter stny. 1/a, H-1117 Budapest, Hungary

Paul N. M. Hoang and Sylvain Picaud

Institut UTINAM−UMR CNRS 6213, Faculté des Sciences, Université de Franche-Comté, F-25030 Besançon Cedex, France

Mihaly Mezei

Department of Structural and Chemical Biology, Mount Sinai School of Medicine, NYU, New York, New York 10029

Received: March 12, 2007; In Final Form: April 14, 2007

The solvation free-energy profiles of 15 different small solutes (i.e., Ar, HF, H_2O, H_2S, NH_3, CH_4, CH_2F_2, CH_2Cl_2, $CHCl_3$, methanol, formaldehyde, formic acid, CO_2, acetone, and acetonitrile) have been calculated across the water/vapor and ice/vapor interfaces by means of Monte Carlo simulations and cavity insertion Widom (CIW) calculations. The CIW calculations have been performed using a new, efficiently parallelized algorithm, which can provide linear speedup on a large number of processors in a distributed memory system. All the solutes considered show preference for being adsorbed at the surface of both liquid water and ice. The free-energy gain of this adsorption relative to the isolated state of the solute molecule is found to be independent of the state (i.e., liquid versus frozen) of the condensed phase, and it is larger for solutes that are able to form stronger or more hydrogen bonds with the water molecules at the surface. On the other hand, the free-energy gain of the adsorption from the bulk liquid phase is found to be stronger for solutes exhibiting stronger amphiphilic character. The solvation free energy of all the solutes studied is found to be considerably higher in ice than in bulk liquid water. The results obtained have several implications on the chemistry of the atmosphere, which are also discussed in the paper.

1. Introduction

The transport of molecules across the liquid/vapor or the solid/vapor interfaces of water is a fundamental process that is important in a wide range of natural phenomena, covering fields from analytical and solution chemistry to atmospheric sciences. Thus, for example, uptake of trace gas molecules by aqueous droplets or ice particles in the atmosphere plays a central role in heterogeneous chemical reactions, which are frequently involved in acid deposition, stratospheric ozone depletion, smog formation, and regional climate changes.[1] Indeed, atmospheric gases that adsorb at the surface of a liquid or solid aerosol particle may diffuse into this particle and participate in heterogeneous chemical reactions with other species there. The reaction products may remain inside the droplet, where they modify the physico-chemical properties of the aerosol, or be released back to the gas phase to participate in further chemistry.

The characterization of the corresponding molecular mechanisms at the interface of the (liquid or solid) aerosol particle with the gas phase (e.g., adsorption, trapping, penetration, and subsequent diffusion) is then of fundamental importance to the understanding of the variety of heterogeneous physico-chemical processes in the stratosphere and upper troposphere and of the interfacial chemistry on snowflakes, ice, and on other water- or ice-covered particles in the atmosphere.

Despite this strong interest (e.g., in atmospheric chemistry), the study of the gas/water or the gas/ice interfaces is relatively recent, because studies of heterogeneous systems are significantly more complex than that of homogeneous ones, both theoretically and experimentally.[2] Nevertheless, from an experimental point of view, a variety of laboratory techniques have been developed in the past 20 years to allow measurements of kinetic parameters for a large number of reactive and nonreactive gas/water(ice) interactions. These kinetic investigations, together with surface sensitive spectroscopic studies and molecular beam experiments, are providing an increasingly detailed and accurate molecular-level understanding of trace gas/water(ice) interfaces.[2,3]

From the theoretical point of view, molecular simulations, such as the molecular dynamics (MD) or the Monte Carlo (MC) method[4] have been used to understand molecular-scale processes at interfaces over short distances (i.e., nanometer length scales) and short times (i.e., nanoseconds time scales).[5] However, most of the theoretical studies, including computer simulations, devoted to the characterization of gas/water or gas/ice interfaces dealt with structural, dynamical, and thermodynamic properties and considered a rather high bulk phase or surface concentration of the solute molecules.[6−14] The difficulty of simulating the

* To whom correspondence should be addressed. E-mail: pali@chem.elte.hu.

10.1021/jp0719816 CCC: $37.00
Published on Web 06/07/2007

transport of a single molecule across an interface is originated in the fact that collecting a statistically relevant sample requires extremely long calculations. The situation is further complicated by the nonequilibrium nature of the process. Thus, several studies in this field consider again systems of relatively high solute concentrations.[15−17]

The thermodynamic driving force of the transport of molecules across interfaces is the gradient of the solvation free energy of the solute along the interface normal axis. Thus, determining the free-energy profile of molecules across the water/vapor or ice/vapor interface can shed light to the thermodynamic background of their transport from one phase to the other. In systems of finite solute concentrations (i.e., when the density of the solute is properly sampled in every regions of the system), the solvation free-energy profile can directly be obtained from the profile of the solute density across the interface. However, at infinite dilution the calculation of solvation free-energy profiles is a computationally far more demanding task than just the generation of an equilibrium sample by computer simulation.[18,19] This difficulty is exacerbated for inhomogeneous systems, such as solid/gas or liquid/gas interfaces, because it lacks the degeneracy that helps to reduce significantly the statistical errors for homogeneous systems. As a result, free-energy profiles calculated with methods that are well tested in homogeneous environment (e.g., free-energy perturbation, thermodynamic integration) may either be affected by large statistical error that makes the results unreliable or require unaffordably long calculations. Instead, free-energy profiles are usually determined[20−37] by potential of mean force (PMF) calculations,[18] employing special methods such as harmonic[38] or adaptive umbrella sampling.[39] In such calculations, the solute molecule is forced to stay at a given (usually rather narrow) region of the system by employing a biasing potential, and the solvation free-energy profile is recovered from the relative frequency of its occurrence at various positions along the interface normal axis. However, to get the full solvation free-energy profile one has to separately explore every, usually 2−5 Å wide slabs of the system along the interface normal, which makes this type of calculation still computationally rather demanding. Thus, there are only a handful of free-energy profile calculations across the liquid water/vapor interface reported in the literature.[5] These calculations led to the general conclusions that small, hydrophilic solutes are usually surface active (i.e., their free energy at the interface is lower than in the bulk), and their free-energy profiles exhibit only small intrinsic barriers (typically less than 1 kcal/mol) for moving the solute from the bulk liquid to the interface.[5] Similar results at the ice/vapor interface are very scarce,[40−44] and the majority of these studies focus on the properties of the various solutes adsorbed at the ice surface,[45−51] although the comparison between the free-energy profiles calculated at liquid and solid interfaces appears to be of fundamental interest for atmospheric sciences, because small changes in the temperature or pressure of the system may result in ice to liquid transformation in the troposphere.

A fast way of calculating solvation free-energy profiles is offered by the test particle insertion method of Widom.[52] In such calculations, the solute molecule is inserted into a set of test points of an equilibrium ensemble of configurations, and the solvation free energy is calculated from the average of the exponential of the interaction energy of the inserted ghost molecule with the rest of the system. Because only the lowest energy test insertions give considerable contribution to this average, both the accuracy and the speed of this calculation can significantly be improved by using the cavity insertion Widom (CIW) variant of the method (i.e., when test insertions are only made into pre-existing cavities of a given minimum radius).[53] The CIW method has recently been successfully applied for the calculation of the solvation free-energy profile of several small molecules across various vapor/liquid and liquid/liquid interfaces[54,55] as well as lipid membrane bilayers.[53,56,57]

The main limitation of the test particle insertion methods comes from the fact that test insertions are only made into configurations that are equilibrated without the presence of the solute molecule. This fact limits the use of the method to uncharged solute molecules of small size. Furthermore, even for such solute molecules the accuracy of the results is not expected to reach the level of those obtained by PMF calculations, when the solvent is allowed to relax around the solute molecule. Nevertheless, in previous studies we compared results of CIW calculations with those of thermodynamic integration and estimated that the error of the CIW calculations is within about 2 kcal/mol in the case of relatively small, neutral solutes (including $CHCl_3$, the largest solute considered in the present study) in an aqueous environment.[53,56] Instead, the main power of the CIW calculation is that it is considerably faster than other methods. In particular, in cases when slowly moving molecules result in a de facto inhomogeneous system the Widom approach, contrary to calculations moving the solute along a single path, averages out the effect of such inhomogeneities. Furthermore, in a CIW calculation the number of the solvent molecule types considered can be increased by relatively little extra computation (because the generation of the equilibrium ensemble of sample configurations and the search for suitable cavities for the test insertions have to be done only once). This feature of the CIW method allows one to compare the interfacial behavior of a large number of molecules as a function of their chemical composition (e.g., noble gases, weak and strong acids, small inorganic molecules of different polarities, alcohols, aldehydes, ketones, chlorofluorocarbons, etc.). Furthermore, as we show in the present paper, the method can be very efficiently parallelized because the analysis of the different sample configurations can be done independently from each other.

In this paper, we present the calculation of the solvation free-energy profile of 15 different solutes (i.e., Ar, HF, H_2O, H_2S, NH_3, CH_4, CH_2F_2, CH_2Cl_2, $CHCl_3$, methanol, formaldehyde, formic acid, CO_2, acetone, and acetonitrile) across the water/vapor and ice/vapor interfaces using a parallelized version of the CIW method. The solutes considered represent a variety of compounds that are present in the atmosphere and are of environmental relevance. Furthermore, their chemical composition is systematically varied in several respects. Thus, among others, the solutes studied include all the differently oxidized derivatives of methane (i.e., CH_4, CH_3OH, HCOH, HCOOH, and CO_2), different chlorinated and fluorinated derivatives of methane (i.e., CH_2F_2, CH_2Cl_2, and $CHCl_3$), the fully hydrogenated derivatives of the elements of the second period (i.e., CH_4, NH_3, H_2O, HF), and also molecules of the same geometry, differing only in the size of one of their atoms (e.g., H_2O and H_2S, CH_2F_2 and CH_2Cl_2).

The paper is organized as follows. In Section 2, a brief description of the CIW method and the details of the calculations performed are given. The parallelization of the computer code that performs the CIW calculation is also described here. The free-energy profiles obtained are presented and discussed in detail in Section 3, whereas in Section 4 the main conclusions of this study are summarized.

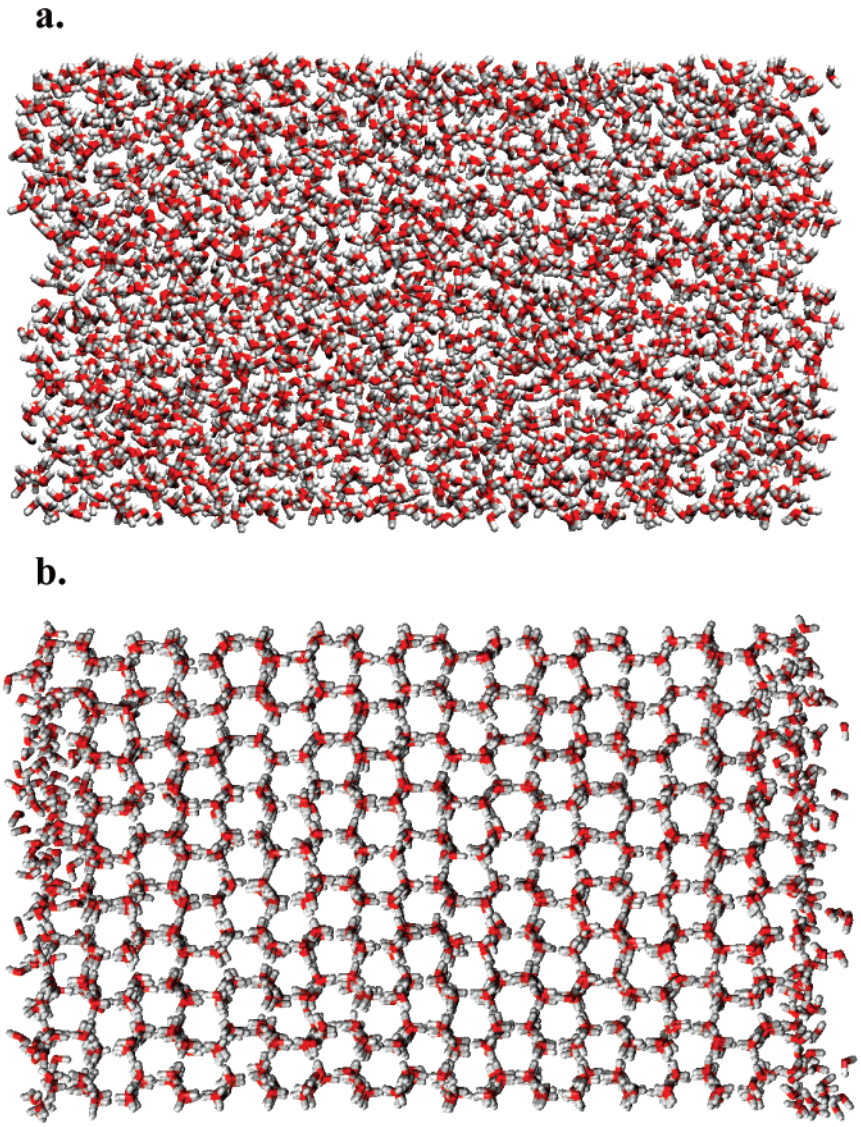

Figure 1. Equilibrated snapshot of (a) the liquid water/vapor and (b) the ice/vapor interfacial system simulated. The O and H atoms of the water molecules are indicated by red and gray colors, respectively.

2. Methods

2.1. The CIW Method. In CIW calculations, the solvation free energy A of the solute molecule of interest is obtained by inserting a test molecule into equilibrated canonical ensemble sample configurations of the system. Insertions are only made into pre-existing cavities (i.e., spherical regions not containing any atomic center) of the minimum radius R_{cav}.[53] A is calculated as

$$A = -k_B T\,[\ln\langle\exp(-U_{test}/k_B T)\rangle + \ln\langle P_{cav}\rangle - 1] - pV/N \quad (1)$$

where U_{test} is the interaction energy of the inserted test particle with the rest of the system, P_{cav} is the probability of finding a cavity of the radius of at least R_{cav}, the brackets <...> denote ensemble averaging, N is the number of the molecules in the system, k_B is the Boltzmann constant, whereas p, V, and T are the pressure, volume, and temperature of the system, respectively. Because at atmospheric and lower pressures the $-pV/N$ term gives only a negligible contribution to the solvation free-energy value, this term is omitted from the calculations presented in this paper. The value of $<P_{cav}>$ can simply be obtained as the ratio of the suitable cavities found and the number of the points checked in the cavity-searching procedure. It should be noted that the speed of the CIW calculation is determined by the cavity-searching procedure, and hence the number of the different solute molecules the free energy of which is calculated can be increased at the expense of relatively little extra computation, given that the same set of cavities is used for all the different solute molecules. Finally, it should be remarked that in the limiting case of $R_{cav} = 0$ Å the value of P_{cav} is unity, and thus the CIW method gives back the original test particle insertion method of Widom.[52]

2.2. Monte Carlo Simulations. To obtain a set of Boltzmann-sampled configurations for the test particle insertions, we have performed Monte Carlo simulations in the canonical (N, V, T) ensemble for the water/vapor and ice/vapor interfacial systems. Both systems contained 2880 water molecules in a rectangular basic simulation box with edge lengths of 100.0, 35.926, and 38.891 Å in the X, Y, and Z directions, respectively (X is the axis perpendicular to the interface.) Standard periodic boundary conditions have been applied. The temperature of the systems containing liquid water and ice has been 300 and 260 K, respectively.

Water molecules have been described by the five-site TIP5P model,[58] which is known to have its freezing point at 274 K[59]

(i.e., very close to that of real water). The interfacial behavior of TIP5P water is known to be rather similar to that of other conventional water models.[60] In creating the starting configuration of the ice/vapor system, 18 molecular layers of proton-disordered I_h ice, containing 160 water molecules per layer, have been placed in the middle of the basic simulation box along the interface normal axis X, using the method of Rick and Haymet.[61] At the beginning of the simulation, the water molecules formed a perfect ice I_h crystal. (The length of the Y and Z axes has been set according to the geometry of this crystal.) The free surface of ice has corresponded to the (0001) basal plane. In the case of the water/vapor system, the starting configuration has been prepared by placing the required number of water molecules randomly in a 62.0 Å × 35.926 Å × 38.891 Å basic simulation box (resulting roughly in the density of liquid water), briefly equilibrating this system through 10^6 Monte Carlo steps, and finally creating the vapor phase by increasing the length of the X edge of the basic box to 100 Å.

The simulations have been performed using the program MMC.[62] In a Monte Carlo step, a randomly chosen water molecule has been randomly translated by no more than 0.25 Å and randomly rotated around a randomly chosen space-fixed axis by no more than 15°. All interactions have been truncated to zero beyond the molecule-based cutoff distance of 12.5 Å. In accordance with the original parametrization of the TIP5P potential model used,[58] no long-range correction has been applied for the electrostatic interactions. The systems have been equilibrated by performing 10^8 Monte Carlo moves. Then, 5000 equilibrium sample configurations per system, separated by 10^5 Monte Carlo moves each, have been saved for the free-energy calculations. To avoid artificial broadening of the interface due to the (energy cost-free) translation of the system along the interface normal axis X during the simulations, the sample configurations have been translated along the X axis by setting the position of the center-of-mass of the system to $X = 0$ Å (i.e., the middle of the simulation box). An equilibrated snapshot of the two systems is shown in Figure 1 for illustration.

2.3. Free-Energy Profile Calculations. We have used the CIW method to calculate the solvation free-energy profile of 15 different solutes (i.e., Ar, HF, H_2O, H_2S, NH_3, CH_4, CH_2F_2, CH_2Cl_2, $CHCl_3$, methanol, formaldehyde, formic acid, CO_2, acetone, and acetonitrile) across the water/vapor and ice/vapor interfaces. All the potential models used to describe the solute molecules are rigid, representing the intermolecular interactions of the molecules as the sum of the interactions of their fractional charges and Lennard-Jones centers, located usually at their different atoms, with the rest of the system. The CH group of the chloroform and CH_3 group of the acetone, acetonitrile and methanol molecules have been treated as united atoms. In the case of the HF and H_2S models, one, whereas in the case of H_2O two equivalent non-atomic interaction sites, denoted here by X, have also been used. The references to the papers where the applied potential models are originally described as well as the geometry and interaction parameters (i.e., the Lennard-Jones distance and energy parameters σ and ϵ, respectively, and the partial charges q) of these models are summarized in Tables 1 and 2.

The free-energy profiles have been calculated using a newly parallelized version of the program MMC.[62] Details of the parallelization of the code are given in the following subsection. The use of the cavity insertion method instead of the original, unbiased Widom-type test particle insertion makes the entire procedure faster, and also the results obtained are more accurate in condensed phases. However, applying the CIW method to the vapor phase would be unnecessary, because in this case practically all the test points are cavity centers and the needless cavity-searching procedure requires a large and unnecessary computing effort. Therefore, we have limited our CIW calculations to the condensed phase of the systems investigated (i.e., to the X range between −35 and 35 Å). In addition, we have performed a conventional Widom calculation (i.e., without searching for cavities) across the entire simulation box in both systems and have used the $|X| > 35$ Å part of the profiles calculated this way to extend the CIW results to the vapor phase as well. This method of combining the CIW and conventional Widom calculation results in determining free-energy profiles across interfaces between a condensed and a vapor phase is described in detail in a previous paper.[54]

TABLE 1: References and Geometry Parameters of the Potential Models Used for the Studied Solutes

solute	reference	bonds formed by	bond length (Å)	angle formed by	bond angle (deg)
Ar	63				
HF	64[a]	F-H	0.973	H-X-F	180.0
		F-X	0.1647		
H_2O	58[b]	O-H	0.9572	H-O-H	104.5
		O-X	0.70	X-O-X	109.5
H_2S[c]	65[d]	S-H	1.3322	H-S-H	92.1
		S-X	0.1933	H-S-X	46.05
NH_3	66	N-H	1.012	H-N-H	106.7
CH_4	67[e]	C-H	1.111	H-C-H	109.5
CH_2F_2	68	C-H	1.09	H-C-H	113.6
		C-F	1.36	F-C-F	108.6
CH_2Cl_2	69	C-H	1.09	H-C-H	109.5
		C-Cl	1.77	Cl-C-Cl	109.5
$CHCl_3$	70[f]	CH-Cl	1.758	Cl-CH-Cl	111.3
methanol	71	CH_3-O	1.425	CH_3-O-H	108.5
		O-H	0.945		
formaldehide[c]	72[f]	C-H	1.101	H-C-H	116.5
		C=O	1.203	H-C=O	121.8
		C-H	1.096	H-C=O	125.5
formic acid[c]	73	C=O	1.213	H-C-O	109.4
		C-O	1.350	O=C-O	125.1
		O-H	0.980	C-O-H	106.1
CO_2	74	C=O	1.230	O=C=O	180.0
acetone[c]	75	CH_3-C	1.507	CH_3-C-CH_3	117.1
		C=O	1.222	CH_3-C=O	121.4
acetonitrile	76[f]	CH_3-C	1.458	CH_3-C≡N	180.0
		N-H	1.157		

[a] JV-NP model. [b]TIP5P model. [c]Molecule of planar geometry. [d]4PCLJ model. [e]CHARMM model. [f]OPLS model.

In the CIW calculations, the explored (i.e., $|X| < 35$ Å) part of the systems has been divided into 25 slabs, each of them being 2.8 Å wide, along the interface normal axis X, and the solvation free-energy values have been calculated in each slab independently. Cavities of the minimum radius of $R_{cav} = 2.8$ Å have been searched for along five different grids, generated by periodically repeated shifts by 0.2 Å along the Y and Z axes. Each grid has contained 100 × 50 × 50 grid points, thus, a total number of 5×10^4 grid points per slab have been checked in every sample configuration. Once a suitable cavity has been found, each test particle has been inserted into it in five different, randomly chosen orientations. In the conventional Widom calculations, the entire systems have been divided into 25 slabs of the width of 4 Å each along the interface normal axis X. Test insertions have been made in randomly chosen orientations at the position of the points of four different, 100 × 10 × 10 grids (i.e., into 1600 points per slab in each configuration). Finally, the profiles obtained have been averaged over the two interfaces present in the system.

2.4. Parallelization of the Widom Calculation. The calculations requiring the analysis of full configurations read from a

TABLE 2: Interaction Parameters of the Potential Models Used for the Solutes Studied

molecule	atom	σ/Å	(ϵ/k_B)/K	q/e
Ar	Ar[a]	3.405	119.9	0.000
HF	F[a]	2.830	60.0	+0.592
	H	0.000	0.0	+0.592
	X	0.000	0.0	−1.184
H_2O	O[a]	3.120	80.6	0.000
	H	0.000	0.0	+0.241
	X	0.000	0.0	−0.241
H_2S	S[a]	3.690	269.0	+0.661
	H	0.000	0.0	+0.278
	X	0.000	0.0	−1.217
NH_3	N[a]	3.385	170.0	−1.035
	H	0.000	0.0	+0.345
CH_4	C[a]	3.671	40.3	−0.360
	H	2.352	11.08	+0.090
CH_2F_2	C[a]	3.150	54.6	+0.300
	F	2.975	40.0	−0.225
	H	2.170	10.0	+0.075
CH_2Cl_2	C[a]	3.350	51.0	+0.022
	Cl	3.350	175.0	−0.109
	H	2.750	13.4	+0.098
$CHCl_3$	CH[a]	3.800	40.3	+0.420
	Cl	3.470	201.4	−0.140
methanol	CH_3[a]	3.740	105.1	+0.265
	O	3.030	86.5	−0.700
	H	0.000	0.0	+0.435
formaldehyde	C[a]	3.750	52.9	+0.450
	O	2.960	105.8	−0.450
	H	2.420	7.6	0.000
formic acid	C[a]	3.727	45.2	+0.445
	O[b]	2.674	146.0	−0.432
	O[c]	3.180	47.1	−0.553
	H[d]	0.800	2.4	+0.107
	H[e]	0.994	12.0	+0.433
CO_2	C[a]	3.262	61.9	+0.663
	O	3.014	97.7	−0.3315
acetone	CH_3	3.748	104.3	0.000
	C[a]	3.360	39.7	+0.565
	O	3.100	67.4	−0.565
acetonitrile	CH_3	3.775	104.1	+0.150
	C[a]	3.650	75.5	+0.280
	N	3.200	85.5	−0.430

[a] Molecular center, placed to the center of the cavity in the insertions. [b]Oxygen double bonded to C. [c]Oxygen of the OH group. [d]Hydrogen chemically bonded to C. [e]Hydrogen of the OH group.

simulation trajectory lend themselves to an efficient coarse-grained parallelization requiring negligible amount of communication. For a computation using N processors, the calculations proceed as follows:

1. All accumulators are initialized in each processor.
2. The master node reads cN structures from the trajectory file.
3. The master node next sends $c(N-1)$ structures to the $N-1$ slave processors, c structures to each.
4. Each processor performs the analysis required (e.g., the insertion attempts) on the c structures.
5. If the results calculated so far needed to be printed or a checkpoint file is needed to be saved, then all slave processor accumulators are summed (reduced) into the corresponding accumulator on the master node, and all the slave accumulators are reinitialized. Results from the master node can be printed or saved.
6. When all processors completed the calculation and there are more structures to be analyzed, the procedure returns to step 2.

The advantage of implementing the parallelization over entire configurations is that there is no need for interprocessor communication during the analysis of a configuration. As a result, the parallel efficiency is not dependent on the various parameters of the analysis or the size of the system. Because the only communication needed involves a large block of data (the full configuration), the parallelization is largely unaffected by latency and thus remains efficient on distributed memory systems. Reading and broadcasting multiple (c) copies is of significance when the time required for the calculation on a structure is not constant because that would reduce the waiting time per structure due to this time variation. In the present implementation, $c = 1$ was chosen, because the CIW calculation times are nearly constant.

For constant calculation time per structure, the speedup S can be calculated as

$$S = \frac{N(t_r + t_c)}{N(2t_r + t_c)} = \frac{N\frac{t_r}{t_c} + N}{N\frac{2t_r}{t_c} + 1} \qquad (2)$$

where N is the number of processors, and t_r and t_c are the times required to read a structure and perform the calculations requested in a structure, respectively. The factor of 2 in the denominator is the result of assuming that sending a structure across the network takes about the same time as reading it into the master node. Thus, as long as the relation $N(t_r/t_c) \ll 1$ holds, S will be close to N. If t_c varies from structure to structure, then S has to be reduced by a factor representing the ratio of the minimum and maximum calculation times. The calculations were run on an Apple G5 cluster using fast ethernet, where for our system we found $t_r = 0.04$ s and $t_c = 37.5$ min, resulting in the t_r/t_c ratio of about 2×10^{-5}. This suggests that the speedup will be close to linear for $O(100)$ processors. Indeed, the whole calculation on ice using the CIW method took 3300 min on 60 processors, representing a speedup of 57. The 5% loss compared to the linear speedup is because the number of cavities varies slightly from structure to structure, and thus some processors have to wait until all processors complete the calculation on their structure.

3. Results and Discussion

The number density profile of the water molecules and the profile of the probability P_{cav} of finding a cavity of the minimum radius of 2.8 Å across the two interfaces considered are shown in Figure 2 as obtained from the Monte Carlo simulations. Contrary to the free-energy profiles, these profiles have been calculated by averaging the water density and P_{cav} values in 0.5 Å rather than 2.8 Å wide slabs along the interface normal axis X. All the profiles shown are symmetrized over the two interfaces present in the basic simulation box. As shown, in bulk liquid water the density of both the water molecules and the cavities are constant along the interface normal axis, whereas at the interface the density of the water molecules drops smoothly to zero within an about 5 Å wide interval. From the X value at which the water density starts to drop, the $P_{cav}(X)$ profile increases rapidly and reaches the value of 1 at the vapor side of the interface. In the ice phase, the water density profile shows nine distinct peaks, corresponding to the nine molecular layers of I_h ice that are present at one side of the simulation box. The $P_{cav}(X)$ profile correlates well with the density profile, showing peaks between the ice layers. The X value at which this profile starts to sharply increase (i.e., the point where the bulk phase of ice ends and the region of the interface begins) is somewhat (i.e., by about 2.5 Å) farther from the middle of

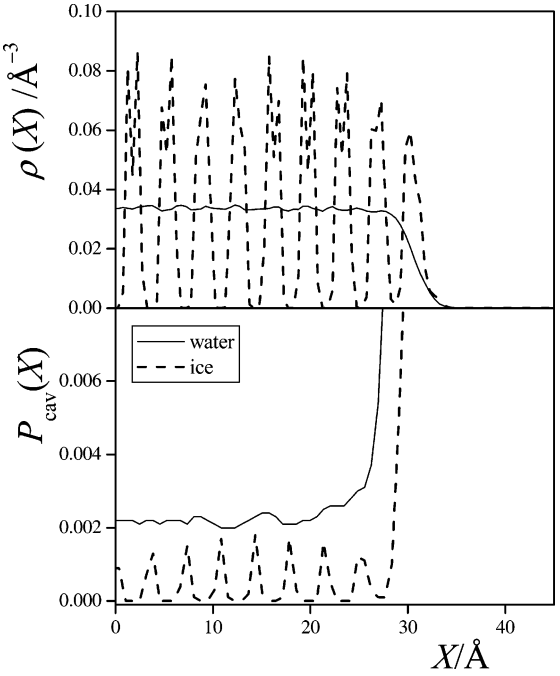

Figure 2. Molecular number density profile of the water molecules (top panel), and probability of finding cavities with the minimum radius of 2.8 Å (bottom panel) along the interface normal axis X across the liquid water/vapor (solid lines) and ice/vapor (dashed lines) interfaces. All the profiles shown are symmetrized over the two interfaces present in the basic simulation box.

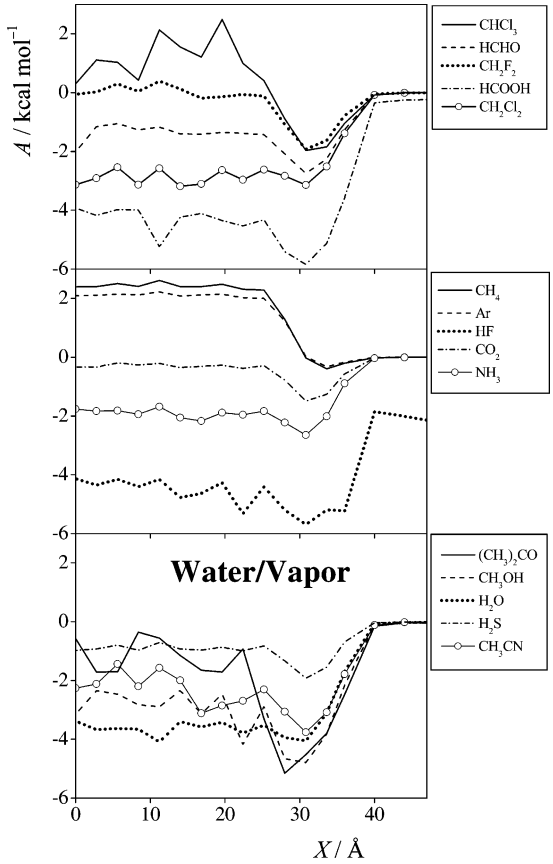

Figure 3. Solvation free-energy profile of the 15 different solute molecules studied along the interface normal axis X across the liquid water/vapor interface. Top panel: chloroform (solid line), formaldehyde (dashed line), difluoromethane (dotted line), formic acid (dash-dotted line), and dichloromethane (open circles). Middle panel: methane (solid line), argon (dashed line), HF (dotted line), CO_2 (dash-dotted line), and ammonia (open circles). Bottom panel: acetone (solid line), methanol (dashed line), water (dotted line), H_2S (dash-dotted line), and acetonitrile (open circles). All the profiles shown are symmetrized over the two interfaces present in the basic simulation box.

the simulation box than in the case of liquid water because the density of bulk liquid water is higher than that of I_h ice. It also shows that the probability of finding an empty cavity of the minimum radius of 2.8 Å is always lower in ice than in liquid water, even between the adjacent layers of the molecules in the ice crystal. This means that although the total volume of the empty space between the molecules is larger in ice than in water (because the ice density is lower than that of water), the distribution of this empty volume shows considerably larger fluctuations in the disordered than in the ordered phase of water.

The free-energy profiles of the 15 solute molecules considered across the water/vapor and ice/vapor interfaces are shown in Figures 3 and 4, respectively, as obtained from the CIW calculations. All the profiles shown are again symmetrized over the two interfaces of the basic simulation box. As shown, all the profiles (with the exception of that of H_2O at the liquid water/vapor interface) show a well-defined minimum between the condensed and vapor phases at the position of the interface, indicating the general ability of these small solute molecules to be adsorbed at these interfaces. In the vapor phase, the vast majority of the profiles drop rapidly to zero, indicating that at the distance of about 10−15 Å from the interface the interaction of the single solute molecule with the bulk-condensed phase of water is already negligible. However, the obtained free-energy profiles of the HF and formic acid molecules behave in a somewhat different way at the water/vapor interface. Thus, at the middle of the vapor phase of the system simulated the solvation free energy of these molecules is still found to be about −2.0 and −0.2 kcal/mol, respectively. The reason of this behavior is that these molecules are characterized by rather large dipole and quadrupole moments, and hence even from a distance of 10−15 Å they can noticeably interact with the charge distribution of the interfacial water molecules. Obviously, at large enough distances the solvation free energy of these solute molecules should also drop to zero, hence, the observed nonzero values at the middle of the vapor phase should be regarded as the consequence of the finite size of the simulation box. One should note that similarly slow (linear) damping of the solvation free-energy profiles of strongly dipolar molecules was observed around fully hydrated bilayers of phospholipid membranes, containing a layer of zwitterionic groups.[56] Interestingly, in the case of the ice/vapor interface even the free-energy profiles of HF and formic acid drop to zero within the simulation box. This is because the symmetry of the ice crystal largely reduces the interaction energy of the interfacial molecules with the charge distribution of a distant solute.

In the bulk liquid water and ice phases, the profiles obtained are oscillating around a constant value. However, the amplitude of this oscillation is rather different for different solute molecules. Because the solvation free energy of a given solute molecule should be constant across the entire bulk phase, the amplitude of the observed oscillation can serve as a measure of the statistical precision of the calculations. (It should be noted that the free-energy oscillations observed in the ice phase are not expected to reflect the layering structure of the molecules in ice, because the width of the slabs within which the solvation free-energy values have been averaged (i.e., 2.8 Å) is rather close to the distance of two adjacent ice layers of about 3.3 Å.) In analyzing the level of this noise, the following general conclusions can be drawn. The precision of the data obtained

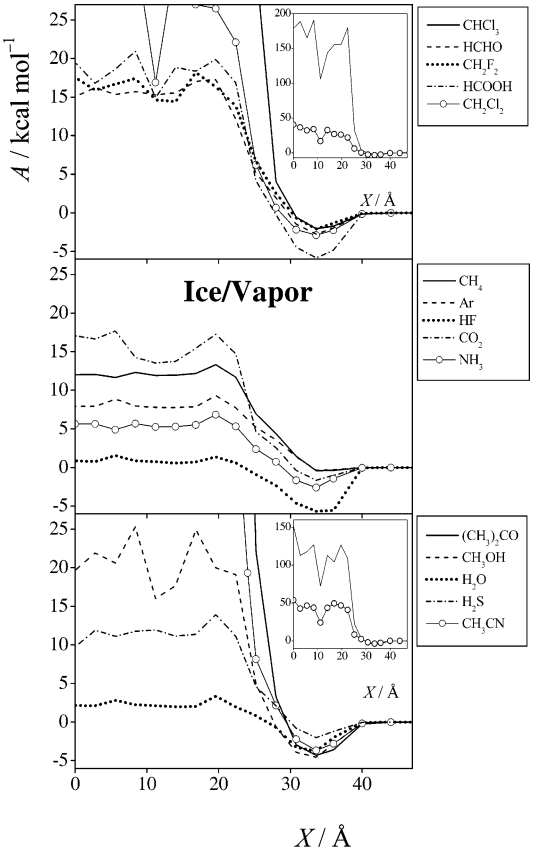

Figure 4. Solvation free-energy profile of the 15 different solutes studied along the interface normal axis *X* across the ice/vapor interface. Notations are the same as in Figure 3. The insets show the profiles of chloroform and dichloromethane (top inset) and of acetone and acetonitrile (bottom inset) on a different scale. All the profiles shown are symmetrized over the two interfaces present in the basic simulation box.

(i) is considerably higher in liquid water than in ice; (ii) it correlates well with the size of the solute molecule, being higher for solutes containing less heavy (i.e., not hydrogen) atoms; and (iii) it is somewhat lower for strongly dipolar (e.g., HF) than for apolar or weakly polar molecules. These findings are originated in the general limitation of the test particle insertion type calculations, i.e., that the test molecules are inserted into previously equilibrated configurations and hence molecules that are expected to strongly modify the local structure of the solvent will find local arrangements for low enough energy test insertions with rather low probabilities. On the basis of the noise in the free-energy profiles obtained, we can estimate that in the bulk liquid phase of water the uncertainty of the data is no more than about ±0.1 kcal/mol for solutes containing only one heavy atom, with the exception of HF and for CO_2; about ±0.2−0.3 kcal/mol for HF and for solutes with two heavy atoms (i.e., methanol and formaldehyde); about ±0.5 kcal/mol for solutes with three heavy atoms (i.e., CH_2Cl_2, formic acid, and acetonitrile); and about ±1 kcal/mol for the largest solutes considered, containing four heavy atoms (i.e., acetone and chloroform). In the ice phase, these uncertainty values are considerably larger, estimated to be about ±0.5 kcal/mol, ±0.5 kcal/mol, ±10 kcal/mol, and ±25−40 kcal/mol for the above four groups of solutes, respectively. This means that the results for the largest solute molecules in ice has to be regarded as semiquantitative data only.

To characterize the ability of the solute molecules considered for being adsorbed at the interface and for being solvated in the bulk-condensed phase, we have calculated the solvation free-energy A^{solv} of the different solutes by averaging the profiles obtained within the *X* range of $|X| \leq 22$ Å according to eq 1, and determined the free energy of their adsorption A^{ads}_{cond} as the difference of A^{solv} and the free-energy value corresponding to the minimum of the free-energy profile at the interface A^{ads}_{vap}. Because of this definition, the simple relation of

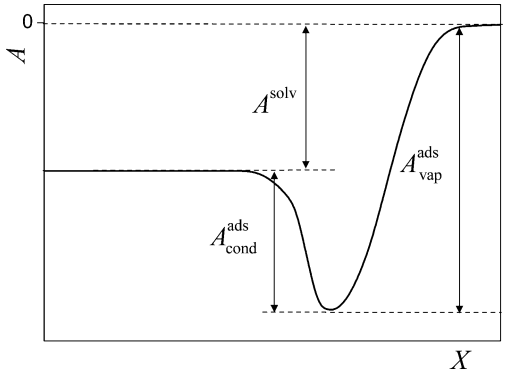

Figure 5. Schematic illustration of the solvation free-energy A^{solv} and adsorption free energies A^{ads}_{cond} and A^{ads}_{vap}.

$$A^{solv} + A^{ads}_{cond} = A^{ads}_{vap} \quad (3)$$

holds between the above free-energy values. Thus, A^{ads}_{cond} and A^{ads}_{vap} represent the free-energy change accompanying the adsorption of the solute molecule at the interface from the bulk-condensed phase and from the vapor phase, respectively. Conversely, $-A^{ads}_{cond}$ and $-A^{ads}_{vap}$ represent the free-energy barrier the solute molecule has to go through upon entering to the bulk-condensed phase from the vapor, and upon leaving the bulk-condensed phase being released to the vapor phase, respectively. Finally, A^{solv} is the solvation free-energy difference between the condensed and vapor phases. (Note that in this calculation, the solvation free-energy value in the vapor phase is regarded to be zero in every case, even for HF and formic acid, for which the nonzero values obtained in the middle of the vapor phase are regarded to be the consequence of the finite size of the vapor phase in the simulation box.) The definition of A^{solv}, A^{ads}_{cond}, and A^{ads}_{vap} is illustrated schematically in Figure 5, whereas the A^{solv}, A^{ads}_{cond}, and A^{ads}_{vap} values obtained for the 15 different solute molecules at the two interfaces considered are summarized in Table 3. Experimental values of A^{solv} and A^{ads}_{cond} are also indicated for comparisons whenever possible. It is seen that, similar to the results of solvation free-energy calculations with the PMF method,[5] the calculated values of A^{solv} agree with the experimental data within about 2 kcal/mol in every case. Much better agreement (i.e., within a 0.1−0.7 kcal/mol) is obtained for the adsorption free-energy values A^{ads}_{cond}. Also note that in the present simulation, the proton configuration in the ice phase has not been changed. Although we do not expect that the neglect of such changes leads to a considerable systematic error of the values of A^{solv} in ice, these values might be somewhat underestimated because of this fact.

When comparing the free-energy profiles as well as solvation and adsorption free-energy values of the different solutes in the water/vapor system, it is evident that all the characteristics depend on the size and polarity of the solute molecule. Thus, the solvation free-energy values of the apolar Ar, CH_4, and of the weakly polar $CHCl_3$ molecules are positive, and their A^{ads}_{vap} values are rather small in magnitude, indicating that these molecules interact only rather weakly with water droplets; they might be weakly bound at the surface (although the adsorption

TABLE 3: Solvation Free Energy and Adsorption Free Energy Values Obtained for the Different Solutes Studied (Experimental Data Are Given in Parenthesis for Comparisons)

	liquid water (kcal/mol)			ice (kcal/mol)		
	A^{solv}	A^{ads}_{cond}	A^{ads}_{vap}	A^{solv}	A^{ads}_{cond}	A^{ads}_{vap}
Ar	2.1 (2.0)[a]	−2.5	−0.4	8	−8.3	−0.4
HF	−4.4	−1.3	−5.7	0.8	−6.5	−5.7
H_2O	−3.7 (−6.3)[a]	0.0 (−0.7)[b]	−3.7	2.2	−5.9	−3.7
H_2S	−0.9	−1.0	−1.9	11	−13	−2.0
NH_3	−1.9 (−4.3)[a]	−0.7 (−0.75)[c]	−2.6	5.4	−8.0	−2.6
CH_4	2.4 (2.0)[a]	−2.8	−0.4	11	−12	−0.4
CH_2F_2	0.03	−2.0	−2.0	15	−17	−2.1
CH_2Cl_2	−3.0	−0.2	−3.2	18	−21	−2.9
$CHCl_3$	1.0	−3.0	−2.0	107	−109	−2.1
methanol	−3.2 (−5.1)[a]	−1.6 (−1.5)[d]	−4.8	17	−22	−4.6
formaldehyde	−1.4	−1.4	−2.8	13	−16	−2.8
formic acid	−4.5	−1.4 (−1.6)[d]	−5.9	16	−22	−5.8
CO_2	−0.3	−1.2	−1.5	14	−16	−1.7
acetone	−1.4	−3.8	−5.2	74	−78	−4.3
acetonitrile	−2.5	−1.3	−3.8	25	−29	−3.7

[a] Ref 77. [b] Ref 78. [c] Ref 79. [d] Ref 80.

free energy of Ar and CH_4 is even smaller than the average thermal energy of the molecules of k_BT), but they are not expected to penetrate into the liquid phase. On the other hand, the strongly polar, hydrophilic solutes, such as HF, NH_3, formic acid, methanol, and acetonitrile, are characterized by large negative A^{solv} values, indicating their ability for being solvated in the liquid phase. Interestingly, the weakly polar CH_2Cl_2 molecule behaves in a rather similar way. Furthermore, CH_2Cl_2 can penetrate into the liquid-phase practically without any free-energy barrier, as the A^{ads}_{cond} value obtained for this molecule is again smaller than the value of k_BT of about 0.6 kcal/mol.

The adsorption ability, characterized by the value of A^{ads}_{cond}, is higher for molecules exhibiting amphiphilic character. Thus, the lowest (i.e., largest in magnitude) A^{ads}_{cond} value is obtained for acetone, a molecule containing a strongly dipolar C═O and two apolar CH_3 groups. Similarly, low A^{ads}_{cond} values are resulted for methanol and acetonitrile, both containing a dipolar part and a CH_3 group. (Although the hydrophobic solutes are also characterized by rather low A^{ads}_{cond} values, this fact is of minor importance, because these molecules are not expected to appear in noticeable concentration in the bulk liquid phase of water.) For water, as is expected, the A^{ads}_{cond} value is resulted in zero. Correspondingly, the solvation free-energy values A^{solv} are deeper for dipolar molecules containing less hydrophobic sites. Thus, the A^{solv} value obtained for water is lower, whereas that obtained for acetone is considerably higher than that of acetonitrile or methanol. The A^{solv} value of acetone is rather close to zero within the estimated uncertainty of the data. This is in accordance with the fact that the free-energy change accompanying the mixing of acetone with water, although negative in all proportions, is rather small.[81−84] Also note that in contrast with water−methanol mixtures of finite concentrations,[6,13] the free-energy profile of methanol at infinite dilution does not show any methanol depletion region. This finding can be explained by the fact, observed both experimentally[85] and from computer simulations,[13] that such a methanol depletion layer builds up at intermediate (i.e., 25−50%) bulk-phase methanol concentrations, whereas only a small remain of it can be detected in systems of smaller methanol content.

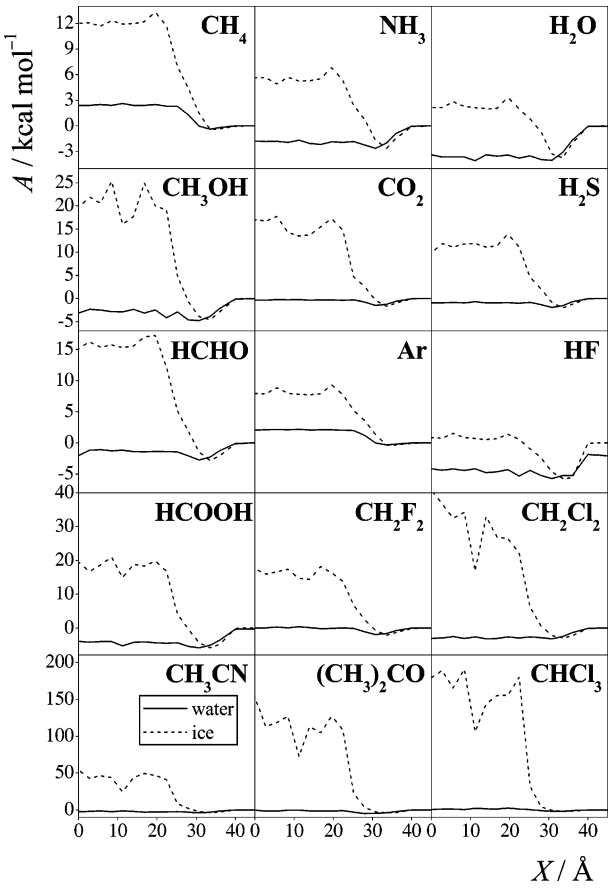

Figure 6. Comparison of the solvation free-energy profile of the 15 different solutes considered as obtained across the water/vapor (solid lines) and ice/vapor (dashed line) interfaces.

The weakly polar H_2S and CH_2F_2, and not dipolar but quadrupolar CO_2 molecules, are characterized by solvation free-energy values that are rather close to zero (the A^{solv} value of CO_2 and CH_2F_2 deviates less from zero than the average thermal energy of the molecules of k_BT). For CO_2, a similar small solvation difference was previously found between condensed aqueous and apolar hydrocarbon phases.[53,56,57] In the case of CO_2 even the adsorption free-energy value is found to be relatively small, indicating that this molecule can be distributed nearly uniformly along the surface normal axis.

The free-energy profiles obtained across the interface between ice and vapor, shown in Figure 4, exhibit a somewhat different behavior than those at the water/vapor interface. A comparison of the profiles obtained for the 15 solute molecules considered at the two different interfaces are shown in Figure 6. The most apparent difference between the two sets of profiles is that they always show considerably higher solvation free-energy values in the ice than in the water phase. Thus, the value of A^{solv} is found to be positive for all the solutes considered in the case of the ice/vapor system. This finding is in accordance with the observed differences of the $P_{cav}(X)$ profiles obtained in the two different systems, namely that water contains considerably more pre-existing cavities that are large enough to accommodate a small solute molecule than ice does. This difference in the structure of the empty space gives rise to the steric hindrance of the solvation of various solutes in the ordered ice phase, even if its density is lower than that of water. Furthermore, a solute molecule can considerably more easily modify the local structure of the surrounding water molecules in liquid water than in ice,

where the well-defined local structure is stabilized by the symmetry of the crystal.

Consistently, the value of A^{solv} is found to be the lowest for the smallest molecules of large dipole moment, i.e., HF, for which A^{solv} is in the order of k_BT, H_2O, and NH_3, because these molecules can be relatively easily accommodated in the cavities existing in the ice crystal and in certain orientations can favorably interact there with the local electric field. It should be noted that, contrary to these molecules, rather large (positive) solvation free-energy values are expected for ions in ice, because the orientational order of the water molecules is imposed by the crystal structure, which has to be thus broken for making favorable interactions with the solvated ion. This difference of the observed small solvation free energy of the neutral HF molecule and expected large solvation free energy of its ions might explain that, despite its strongly acidic character, HF is known to exist in its molecular form in ice.[86−88] The apolar or weakly polar solutes that contain only one heavy atom (i.e., Ar, CH_4, and H_2S) are characterized by somewhat larger solvation free-energy values, scattering around 10 kcal/mol, whereas for the solutes containing two or three heavy atoms the value of A^{solv} is found to be between 13 and 25 kcal/mol. Finally, the highest solvation free-energy values are obtained for the largest solutes considered (i.e., acetone and chloroform); however, in this case the obtained values of A^{solv} are affected by rather large statistical uncertainties, which prevents us from drawing further conclusions.

Since the value of A^{solv} is found to be positive for all solutes considered, indicating that all these molecules prefer to stay in the vapor phase rather than penetrating into the ice, their ability for being adsorbed at the interface is characterized by the value of A^{ads}_{vap} rather than A^{ads}_{cond}. Interestingly, the value of A^{ads}_{vap} is found to be practically identical with that in the case of the liquid water/vapor interface for all the solutes studied (see Figure 6 and Table 3). This means that at least some parts of the surfaces of liquid water and ice are characterized by similar local order of the molecules. This finding is consistent with the observed disorder induced by the vicinity of the vapor phase at the surface of ice (see Figure 1).

The adsorption ability of the solutes at the ice/vapor interface depends on the strength of their interaction with water rather than on their size. Thus, the lowest values of A^{ads}_{vap} are obtained for HF and HCOOH (i.e., the molecules that can either form an exceptionally strong or more than one hydrogen bond with water). All the solutes that are able to form a hydrogen bond with the interfacial water molecules are characterized by A^{ads}_{vap} values lower than −2.5 kcal/mol, which is typically lower for solutes that can either be the H-donor or the H-acceptor partner in such bonds than for solutes without H-donating ability (i.e., formaldehyde, acetone, and acetonitrile). Interestingly, CH_2Cl_2 behaves in this respect again very similarly to the strongly polar, hydrogen-bonding solute molecules, having the A^{ads}_{vap} value of −2.9 kcal/mol. However, the adsorption free-energy values of the other non-hydrogen bonding solutes are considerably higher, being above −2 kcal/mol in every case, and they are found to be lower for the weakly polar (i.e., H_2S, $CHCl_3$, CH_2F_2) than for the non-dipolar molecules, and lower for the quadrupolar CO_2 molecule than for the apolar solutes (i.e., Ar and CH_4), for which they are smaller than the average thermal energy of the molecules of k_BT.

4. Summary and Conclusions

In this paper, we have presented the calculation of the solvation free-energy profile of 15 different solutes across the water/vapor and ice/vapor interfaces. This study clearly emphasizes the main merit of the CIW method for such calculations, namely, that although it is less precise than PMF calculations employing umbrella sampling and its use is limited to small solutes of zero net charge, it is rather fast and, in particular, the number of the different solutes considered can be increased without a considerable increase of the required computational cost. Furthermore, it is demonstrated that the algorithm can be very efficiently parallelized, obtaining a linear speedup on a large number of processors in distributed-memory systems. These features make the CIW method particularly suitable for the comparison of the behavior of a large set of different solutes in various systems.

The profiles obtained show the following general features: (i) all solutes considered show preference for being adsorbed at the interface; (ii) the free-energy gain of this adsorption from the bulk liquid phase is stronger for solutes exhibiting stronger amphiphilic character; (iii) the free-energy gain of this adsorption from the vapor phase is stronger for solutes that are able to form stronger or more hydrogen bonds with the water molecules; (iv) the free-energy gain of adsorption from the vapor phase is the same at the surface of liquid water and ice; and (v) the solvation free-energy value in the ice phase is always much larger than in both the liquid water and the vapor phase.

The above conclusions have also several important implications in atmospheric chemistry. Thus, the high value of the solvation free energy in the ice phase for the species considered in the present study is likely to be related to the fully reversible nature of their adsorption on ice, as observed in coated-wall flow tube experiments for nondissociable molecules.[89] Moreover, although the present results show that the precursor stage of the trapping of atmospheric gases (i.e., the surface adsorption) does not depend on the liquid versus solid state of the water substrate, the second stage of the trapping process (i.e., the incorporation into the bulk phase) is energetically far more favorable in the liquid than in the solid phase. As a consequence, the uptake of these atmospheric gases (especially those that are able to form strong hydrogen bonds with water) is certainly larger on water droplets than on ice particles. Then, a small increase in temperature or the presence of impurities in ice, such as ions, can strongly influence the scavenging of the atmospheric trace gases, as shown from recent experiments on doped ice surfaces[90] and supercooled solutions.[91]

Acknowledgment. P.J. is a Békésy György fellow of the Hungarian Ministry of Education, which is gratefully acknowledged. This work has been supported by the MTA-CNRS bilateral collaboration program, and by the Hungarian OTKA Foundation under Project No. T049673. The authors are grateful to Albert Bartók for providing the coordinates of the molecules in the ice I_h crystal.

References and Notes

(1) Finlayson-Pitts, B. J.; Pitts, J. N. *Chemistry of the Upper and Lower Atmosphere*; Academic Press: San Diego, CA, 2000.

(2) Davidovits, P.; Kolb, C. E.; Williams, L. R.; Jayne, J. T.; Worsnop, D. R. *Chem. Rev.* **2006**, *106*, 1323.

(3) Reid, J. P.; Sayer, R. M. *Chem. Soc. Rev.* **2003**, *32*, 70.

(4) Allen, M. P.; Tildesley, D. J. *Computer Simulations of Liquids*; Clarendon Press: Oxford, 1987.

(5) Garrett, B. C.; Schenter, G. K.; Morita, A. *Chem. Rev.* **2006**, *106*, 1355.

(6) Matsumoto, M.; Takaoka, Y.; Kataoka, Y. *J. Chem. Phys.* **1993**, *98*, 1464.

(7) Benjamin, I. *Phys. Rev. Lett.* **1994**, *73*, 2083.

(8) Tarek, M.; Tobias, D. J.; Klein, M. L. *J. Chem. Soc., Faraday Trans.* **1996**, *92*, 559.

(9) Mountain, R. D. *J. Phys. Chem. A* **1999**, *103*, 10744.
(10) Mountain, R. D. *J. Phys. Chem. B* **2001**, *105*, 6556.
(11) Paul, S.; Chandra, A. *J. Chem. Phys.* **2005**, *123*, 184706.
(12) Chang, T. M.; Dang, L. X. *J. Phys. Chem. B* **2005**, *109*, 5759.
(13) Pártay, L.; Jedlovszky, P.; Vincze, Á.; Horvai, G. *J. Phys. Chem. B* **2005**, *109*, 20493.
(14) Pártay, L.; Jedlovszky, P.; Jancsó, G. *Chem. Phys. Lett.* **2006**, *420*, 367.
(15) Troxler, L.; Wipff, G. *Anal. Sci.* **1998**, *14*, 43.
(16) Berny, F.; Schurhammer, R.; Wipff, G. *Inorg. Chim. Acta* **2000**, *300*−*302*, 384.
(17) Schnell, B.; Schurhammer, R.; Wipff, G. *J. Phys. Chem. B* **2004**, *108*, 2285.
(18) Mezei, M.; Beveridge, D. L. *Ann. N.Y. Acad. Sci.* **1986**, *482*, 1.
(19) Straatsma, T. P.; McCammon, J. A. *Annu. Rev. Phys. Chem.* **1992**, *43*, 407.
(20) Pohorille, A.; Benjamin, I. *J. Chem. Phys.* **1991**, *94*, 5599.
(21) Pohorille, A.; Benjamin, I. *J. Phys. Chem.* **1993**, *97*, 2664.
(22) Schweighofer, K. J.; Benjamin, I. *J. Phys. Chem.* **1995**, *99*, 9974.
(23) Wilson, M. A.; Pohorille, A. *J. Phys. Chem. B* **1997**, *101*, 3130.
(24) Taylor, R. S.; Ray, D.; Garrett, B. C. *J. Phys. Chem. B* **1997**, *101*, 5473.
(25) Taylor, R. S.; Garrett, B. C. *J. Phys. Chem. B* **1999**, *110*, 844.
(26) Benjamin, I. *J. Chem. Phys.* **1999**, *110*, 8070.
(27) Fernandes, P. A.; Cordeiro, M. N. D. S.; Gomes, J. A. N. F. *J. Phys. Chem. B* **1999**, *103*, 8930.
(28) Fernandes, P. A.; Cordeiro, M. N. D. S.; Gomes, J. A. N. F. *J. Phys. Chem. B* **2000**, *104*, 2278.
(29) Dang, L. X. *J. Phys. Chem. B* **2001**, *105*, 804.
(30) Shin, J. Y.; Abbott, N. L. *Langmuir* **2001**, *17*, 8434.
(31) Dang, L. X. *J. Chem. Phys.* **2003**, *119*, 6351.
(32) Roeslová, M.; Jungwirth, P.; Tobias, D. J.; Gerber, R. B. *J. Phys. Chem. B* **2003**, *107*, 12690.
(33) Dang, L. X.; Garrett, B. C. *Chem. Phys. Lett.* **2004**, *285*, 309.
(34) Vacha, R.; Slavicek, P.; Mucha, M.; Finlayson-Pitts, B. J.; Jungwirth, P. *J. Phys. Chem. A* **2004**, *108*, 11573.
(35) Roeslová, M.; Vieceli, J.; Dang, L. X.; Garrett, B. C.; Tobias, D. J. *J. Am. Chem. Soc.* **2004**, *126*, 16308.
(36) Paul, S.; Chandra, A. *Chem. Phys. Lett.* **2004**, *400*, 515.
(37) Vieceli, J.; Roeslová, M.; Potter, N.; Dang, L. X.; Garrett, B. C.; Tobias, D. J. *J. Phys. Chem. B* **2005**, *109*, 15876.
(38) Pangali, C. S.; Rao, M.; Berne, B. J. *J. Chem. Phys.* **1979**, *71*, 2975.
(39) Mezei, M. *J. Comput. Phys.* **1987**, *68*, 237.
(40) Toubin, C.; Hoang, P. N. M; Picaud, S.; Girardet, C.; Lynden-Bell, R. M. *Surf. Rev. Lett.* **1999**, *6*, 1265.
(41) Toubin, C.; Hoang, P. N. M; Picaud, S.; Girardet, C. *J. Chem. Phys.* **2000**, *113*, 1184.
(42) Toubin, C.; Picaud, S.; Hoang, P. N. M; Girardet, C.; Lynden-Bell, R. M.; Hynes, J. T. *J. Chem. Phys.* **2003**, *118*, 9814.
(43) Picaud, S.; Hoang, P. N. M. *Phys. Chem. Chem. Phys.* **2004**, *6*, 1970.
(44) Mitlin, S.; Lemak, A. S.; Torrie, B. H.; Leung, K. T. *J. Phys. Chem. B* **2003**, *107*, 9958.
(45) Kroes, G. J.; Clary, D. C. *J. Phys. Chem*. **1992**, *96*, 7079.
(46) Buch, V.; Delzeit, L.; Blackledge, C.; Devlin, J. P. *J. Phys. Chem*. **1996**, *100*, 3732.
(47) Al-Halabi, A.; Klein, A. W.; Kroes, G. J. *Chem. Phys. Lett*. **1999**, *307*, 505.
(48) Bolton, K.; Petterson, J. B. C. *Chem. Phys. Lett.* **1999**, *312*, 71.
(49) Uras, N.; Buch, V.; Devlin, J. P. *J. Phys. Chem. B* **2000**, *104*, 9203.
(50) Al-Halabi, A.; Klein, A. W.; Kroes, G. J. *J. Chem. Phys.* **2001**, *115*, 482.
(51) Jedlovszky, P.; Pártay, L.; Hoang, P. N. M.; Picaud, S.; von Hessberg, P.; Crowley, J. N. *J. Am. Chem. Soc.* **2006**, *128*, 15300.
(52) Widom, B. *J. Chem. Phys.* **1963**, *39*, 2808.
(53) Jedlovszky, P.; Mezei, M. *J. Am. Chem. Soc.* **2000**, *122*, 5125.
(54) Jedlovszky, P.; Varga, I.; Gilányi, T. *J. Chem. Phys*. **2003**, *119*, 1731.
(55) Jedlovszky, P.; Vincze, Á.; Horvai, G. *J. Mol. Liq.* **2004**, *109*, 99.
(56) Jedlovszky, P.; Mezei, M. *J. Phys. Chem. B* **2003**, *107*, 5322.
(57) Shinoda, W.; Mikami, M.; Baba, T.; Hato, M. *J. Phys. Chem. B* **2004**, *108*, 9346.
(58) Mahoney, M. W.; Jorgensen, W. L. *J. Chem. Phys*. **2000**, *112*, 8910.
(59) Vega, C.; Abascal, J. L. F. *J. Chem. Phys.* **2005**, *123*, 144504.
(60) Jedlovszky, P.; Předota, M.; Nezbeda, I. *Mol. Phys.* **2006**, *104*, 2465.
(61) Rick, S. W.; Haymet, A. D. J., *J. Chem. Phys.* **2003**, *118*, 9291.
(62) Mezei, M. MMC: Monte Carlo program for simulation of molecular assemblies. http://inka.mssm.edu/~mezei/mmc (accessed May, 2007).
(63) Ruff, I.; Baranyai, A.; Pálinkás, G.; Heinzinger, K. *J. Chem. Phys*. **1986**, *85*, 2169.
(64) Jedlovszky, P.; Vallauri, R. *Mol. Phys.* **1997**, *92*, 331.
(65) Forester, T. R.; McDonald, I. R.; Klein, M. L. *Chem. Phys*. **1989**, *129*, 225.
(66) Kristóf, T.; Vorholz, J.; Liszi, J.; Rumpf, B.; Maurer, G. *Mol. Phys.* **1999**, *97*, 1129.
(67) Schlenkirch, M.; Brickmann, J.; MacKerell, A. D., Jr.; Karplus, M. In *Biological Membranes*; Merz, K. M., Roux, B., Eds.; Birkhäuser: Boston, MA, 1996; pp 31−82.
(68) Jedlovszky, P.; Mezei, M. *J. Chem. Phys*. **1999**, *110*, 2991.
(69) Ferrario, M.; Evans, M. W. *Chem. Phys*. **1982**, *72*, 141.
(70) Jorgensen, W. L.; Briggs, J. M.; Contreras, M. L. *J. Phys. Chem*. **1990**, *94*, 1683.
(71) van Leeuwen, M. E.; Smit, B. *J. Phys. Chem.* **1995**, *99*, 1831.
(72) Jorgensen, W. L.; Maxwell, D. S.; Tirado-Rives, J. *J. Am. Chem. Soc.* **1996**, *118*, 11225.
(73) Jedlovszky, P.; Turi, L. *J. Phys. Chem. A* **1997**, *101*, 2662; (Erratum) **1999**, *103*, 3796.
(74) Somasundaram, T.; in het Panhuis, M.; Lynden-Bell, R. M.; Patterson, C. H. *J. Chem. Phys*. **1999**, *111*, 2190.
(75) Weerasinghe, S.; Smith, P. E. *J. Chem. Phys.* **2003**, *118*, 10663.
(76) Jorgensen, W. L.; Briggs, J. M. *Mol. Phys.* **1988**, *63*, 547.
(77) Ben-Naim, A.; Marcus, Y. *J. Chem. Phys.* **1984**, *81*, 2016.
(78) Li, Y. Q.; Davidovits, P.; Shi, Q.; Jayne, J. T.; Kolb, C. E.; Worsnop, D. R. *J. Phys. Chem. A* **2001**, *105*, 10627.
(79) Shi, Q.; Davidovits, P.; Jayne, J. T.; Worsnop, D. R.; Kolb, C. E. *J. Phys. Chem. A* **1999**, *103*, 8812.
(80) Jayne, J. T.; Duan, S. X.; Davidovits, P.; Worsnop, D. R.; Zahniser, M. S.; Kolb, C. E. *J. Phys. Chem*. **1991**, *95*, 6329.
(81) Matteoli, E.; Lepori, L. *J. Chem. Phys*. **1984**, *80*, 2856.
(82) Blandamer, M. J.; Burgess, J.; Cooney, A.; Cowles, H. J.; Horne, I. M.; Martin, K. J.; Morcom, K. W.; Warrick, Jr., P. *J. Chem. Soc., Faraday Trans* **1990**, *86*, 2209.
(83) Perera, A.; Sokolic, F. *J. Chem. Phys*. **2004**, *121*, 11272.
(84) Perera, A.; Sokolic, F.; Almásy, L.; Westh, P.; Koga, Y. *J. Chem. Phys*. **2005**, *123*, 024503.
(85) Chen, H.; Gan, W.; Lu, R.; Guo, Y.; Wang, H. F. *J. Phys. Chem. B* **2005**, *109*, 8064.
(86) Hanson, D. R.; Ravishankara, A. R. *J. Phys. Chem*. **1992**, *96*, 9441.
(87) Robertson, S. H.; Clary, D. C. *Faraday Discuss.* **1995**, *100*, 309.
(88) Ando, K.; Hynes, J. T. *J. Phys. Chem. A* **1999**, *103*, 10398.
(89) Abbatt, J. P. D. *Chem. Rev*. **2003**, *103*, 4793.
(90) Journet, E.; Le Calve, S.; Mirabel, P. *J. Phys. Chem. B* **2005**, *109*, 14112.
(91) Kerbrat, M.; Le Calve, S.; Mirabel, P. *J. Phys. Chem. A* **2007**, *111*, 925.